ELSEVIER

Infrared brazing Ti–6Al–4V and SP-700 alloys using the Ti–20Zr–20Cu–20Ni braze alloy

C.T. Chang [a], Z.Y. Wu [b], R.K. Shiue [b,*], C.S. Chang [c]

[a] *Department of Mechanical Engineering, National Hualien Industrial Vocational Senior High School, Hualien 970, Taiwan*
[b] *Department of Materials Science and Engineering, National Taiwan University, Taipei 106, Taiwan*
[c] *Engineered Materials Solutions, 39 Perry Avenue, MS 4-1, Attleboro, MA 02703-2410, USA*

Abstract

Great efforts have been made in brazing high-strength α–β titanium alloys below their beta-phase transformation temperature in order to obtain optimized mechanical properties. The brazing temperature of the cold roll-bonded Ti–20Zr–20Cu–20Ni foil is roughly 70 °C lower than that of Ti–15Cu–15Ni filler metal. Moreover, the detrimental Cu–Ni and Cu–Ni–Zr rich Ti phases can be greatly reduced or eliminated by properly choosing the brazing thermal cycle. This research demonstrates the potential application of Ti–20Zr–20Cu–20Ni foil in brazing titanium alloys.
© 2006 Elsevier B.V. All rights reserved.

1. Introduction

Ti–6Al–4V and SP-700 are two-phase α–β titanium alloys, which can be strengthened by proper thermal mechanical treatments [1–3]. Ti–6Al–4V is the most widely used titanium alloy that accounts for approximately 60% of the Ti usage worldwide. SP-700 (4.5% Al, 3% V, 2% Fe and 2% Mo) is a β-rich, α–β alloy developed particularly to yield a superfine microstructure for superplastic forming capability at 700 °C [1].

Brazing of titanium and its alloys became an important joining process during the past decade to meet the increasingly demanding structural applications [4–6]. Titanium brazing for elevated temperature services are frequently brazed with titanium-based filler metals of which Cu and Ni are added as melting point depressants [4,7–9]. Ti–15Cu–15Ni and Ti–15Cu–25Ni are commercially available Ti-based braze alloys. However, it is preferred that the brazing temperature of α–β titanium alloys do not exceed the beta transus temperature, which varies from 900 to 1040 °C to obtain the fine equiaxial duplex microstructure for optimized mechanical properties [4,10].

Brazing temperatures of Ti–Cu–Ni filler metals can be lowered with the addition of Zr in Ti–Cu–Ni alloys. A cold roll-bonding process is applied to combine Ti, Zr, Cu and Ni strip into a layered composite that allows conventional cold rolling process to produce the Ti–20Zr–20Cu–20Ni brazing foil studied here [11]. Additionally, the cold roll-bonding process makes an economic way to produce Ti–20Zr–20Cu–20SNi braze foils for industrial usage.

2. Experimental

Ti–6Al–4V and SP-700 plates measured 10 mm × 7 mm × 3 mm were prepared for the brazing experiments. Ti–20Zr–20Cu–20Ni (in weight percent) foil, 50 μm thick was used as the braze filler, which consisted of Ti, Zr, Cu and Ni layers in the as-rolled condition [11]. Infrared brazing was performed in a vacuum of 5×10^{-5} mbar at 900, 930, 960 and 990 °C from 180 s to 3600 s to study the microstructural evolution of infrared brazed joints. Brazed specimens were sectioned and prepared by standard metallographic procedure for the microstructure examination.

Shear test was performed using a Shimadzu AG-10 universal testing machine at a constant crosshead speed of 0.5 mm/min [10,12]. The fractured surface and cross section were examined

* Corresponding author. Tel.: +886 2 33664533; fax: +886 2 23634562.
E-mail address: rkshiue@ntu.edu.tw (R.K. Shiue).
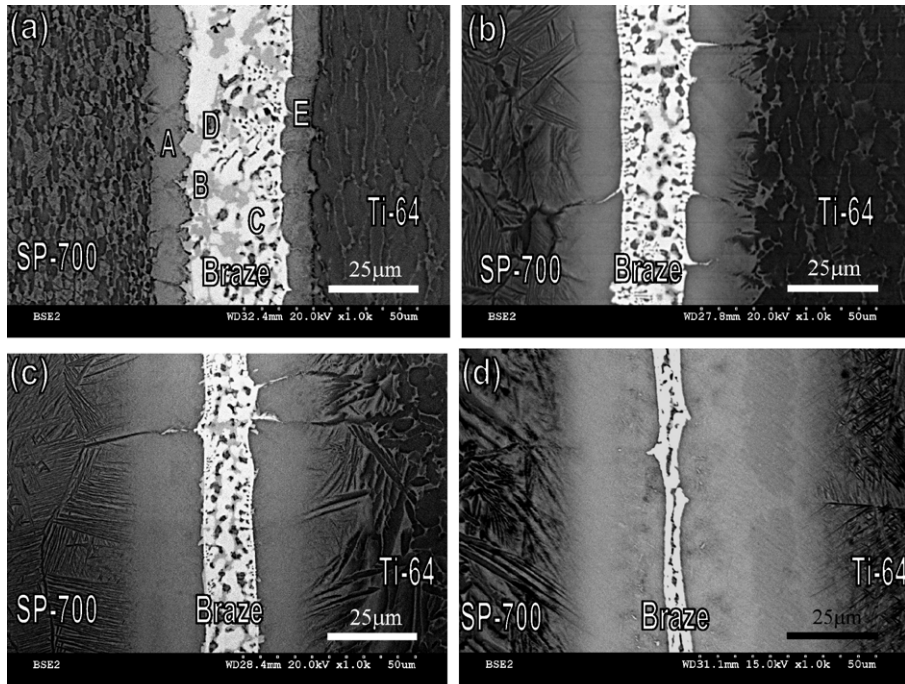
Location	A	B	C	D	E
Ti	79.0	61.1	45.6	84.0	78.5
V	2.7	0.2	1.0	1.6	2.3
Al	5.7	1.3	5.1	3.4	6.2
Zr	2.7	5.8	15.8	3.4	2.8
Cu	4.7	9.5	14.7	3.5	5.1
Ni	4.0	20.8	17.0	3.3	4.6
Mo	0.2	0.0	0.0	0.0	0.1
Fe	1.0	1.2	0.7	0.6	0.4

Fig. 1. SEM BEIs and EPMA chemical analysis results in atomic percent of the infrared brazed specimens with various brazing conditions: (a) 900 °C for 180 s, (b) 930 °C for 300 s, (c) 990 °C for 300 s and (d) 900 °C for 1800 s.
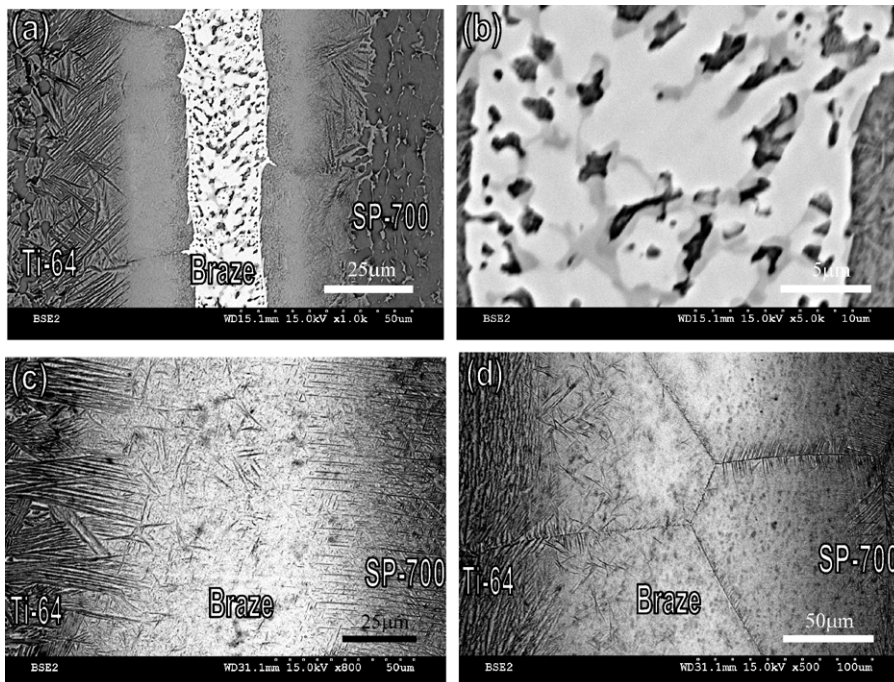

Fig. 2. SEM BEIs of the infrared brazed specimens with various brazing conditions: (a,b) 900 °C for 600 s, (c) 900 °C, for 3600 s and (d) 990 °C for 3600 s.

Table 1
Shear strengths of infrared brazed specimens with various brazing conditions

Temperature (°C)	Time (s)	Average shear strength (MPa)
900	180	220
900	600	326
900	1800	352
900	3600	391
930	180	265
960	180	276
990	180	309
990	3600	483
		(Substrate fracture)

using a Hitachi 3500 H scanning electron microscope (SEM) operated at an accelerating voltage of 15 kV. Quantitative chemical analysis was performed using a JEOL JXA 8200 EPMA with a minimum spot size of 1 μm.

3. Results and discussion

Fig. 1 shows SEM BEIs (backscattered electron images) and EPMA chemical analysis results in atomic percent of infrared brazed specimens with various brazing conditions. The brazed joint consists of three distinctive phases at lower magnifications: (1) Ti-rich phase with low Cu, Ni, Zr contents (marked by A, D and E), (2) Cu–Ni rich Ti phase (marked by B), and (3) Cu–Ni–Zr rich Ti phase (marked by C). The bright white Cu–Ni–Zr rich Ti phase in the backscattered electron image resulted from the high content of Zr in the phase. It is also important to note that the amount of both Cu–Ni and Cu–Ni–Zr rich Ti phases is decreased with increasing brazing temperature and/or time. The width of Cu–Ni–Zr rich Ti phase is decreased below 5 μm for the specimen infrared brazed at 900 °C for 1800 s (Fig. 1(d)).

Fig. 2 illustrates SEM BEIs from specimens with longer brazing time. Cu–Ni and Cu–Ni–Zr rich Ti phases completely disappeared for specimen infrared brazed at 900 and 990 °C for 3600 s, respectively.

The microstructural evolution of brazed joint using Ti–20Zr–20Cu–20Ni alloy is similar to that in the studies of Ti–Cu–Ni fillers [13,14]. Cu–Ni and Cu–Ni–Zr rich Ti phases can be completely eliminated from the brazed joint when high brazing temperatures and/or longer brazing time are applied.

According to binary Cu–Ti and Ni–Ti phase diagrams, the solubility of Cu and Ni in the β-Ti is much greater than that in the α-Ti and a significant amount of Cu and Ni can be absorbed during brazing [15]. Zr is completely miscible with Ti [15]. The diffusion of Cu, Ni and Zr into both Ti alloy substrates is expected and driven by the concentration gradients of these elements in the brazed joint. Accordingly, the disappearance of Cu–Ni–(Zr)–Ti phases in the brazed joint is rate-controlled by diffusion of Cu, Ni and Zr in the Ti substrates. The homogenization of Cu, Ni, Ti and Zr in the brazed joints and the effect of interdiffusion on the substrate microstructure are shown in Figs. 1 and 2.

It was reported that the amount of Cu–Ni rich Ti phase strongly related to the strength of brazed joint [14]. The effect of Cu–Ni and Cu–Ni–Zr rich Ti phases on braze joint strength of Ti–Zr–Cu–Ni filler is evaluated in this experiment to identify if there is any similarity. Table 1 lists the average shear strength of infrared brazed specimens with various brazing conditions. The specimen infrared brazed at 900 °C for 180 s has the lowest shear strength of 220 MPa but increases almost doubled to 391 MPa when brazing time was increased to 3600 s. The specimen infrared brazed at 990 °C for 3600 s has the highest shear strength of 483 MPa, and the fracture propagated in the substrate instead of through the brazed joint.

Fig. 3 shows the cross sections of brazed joints with various brazing conditions after shear test. The fracture path propagated through the brazed joint is observed for the specimen infrared brazed at 900 °C for 180 s and 1800 s (Fig. 3(a,b)). The fracture path changed from the brazed joint to substrate for specimen infrared brazed at 990 °C for 3600 s (Fig. 3 (d)), which also has the highest shear strength of 483 MPa. The shear strength measurements and the fracture behaviors suggest that the presence of Cu–Ni and Cu–Ni–Zr rich Ti phases in the brazed joint is detrimental and they should be avoided in order to obtain a robust joint.
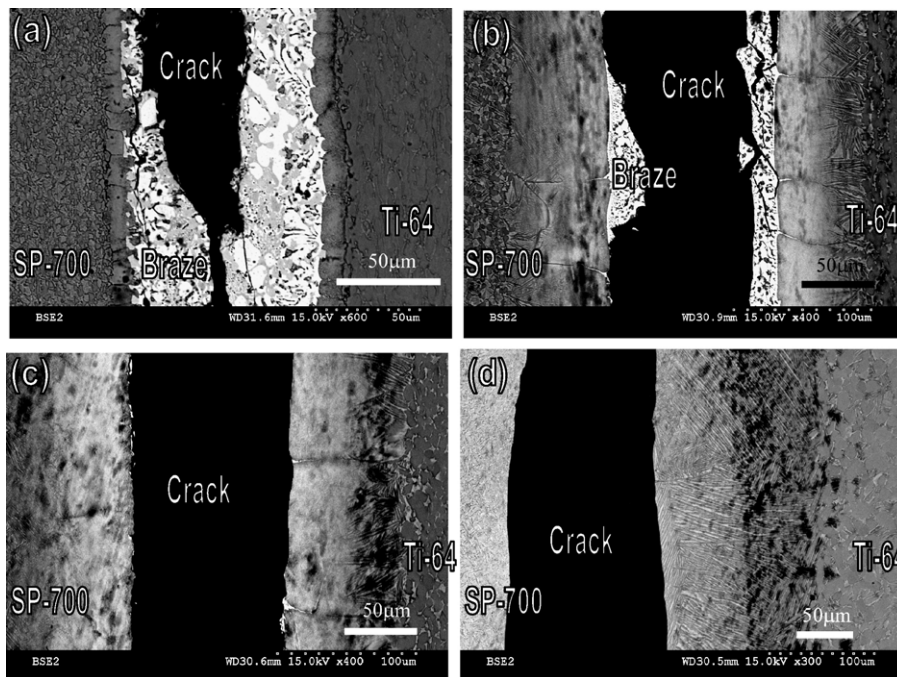

Fig. 3. SEM BEIs displaying the cross section of brazed joints after shear test: (a) 900 °C for 180 s, (b) 900 °C for 1800 s, (c) 900 °C for 3600 s and (d) 990 °C for 3600 s.
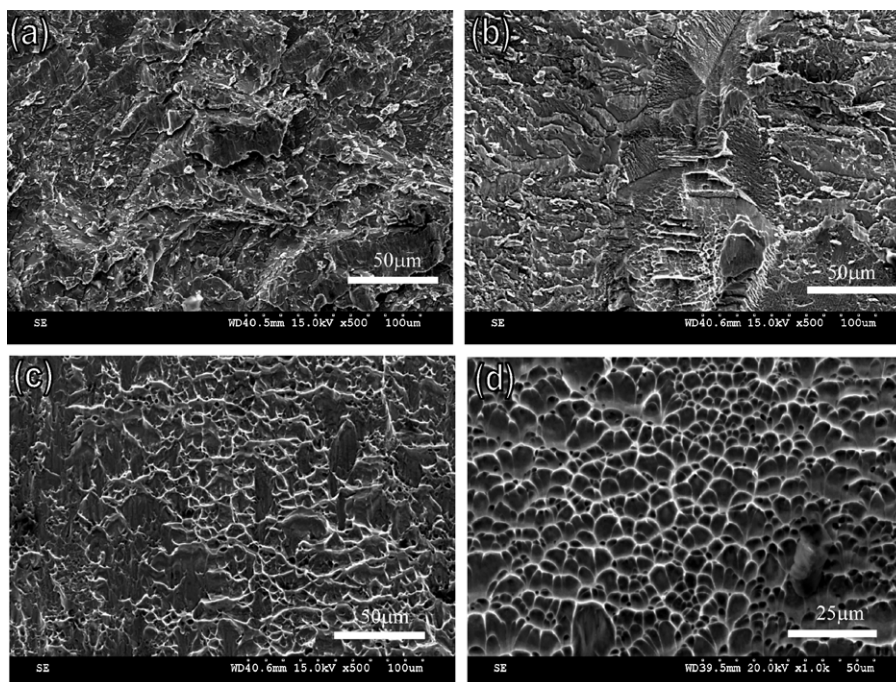
Fig. 4. SEM fractographs of infrared brazed specimens after shear tests: (a) 900 °C for 180 s, (b) 900 °C for 600 s, (c) 900 °C for 3600 s and (d) 990 °C for 3600 s.

Fig. 4 shows SEM fractographs of infrared brazed specimens with different brazing conditions after shear tests. Quasi-cleavage fracture is widely observed in specimens with lower brazing temperature and shorter brazing time, e.g. 900 °C for 180 s and 600 s (Fig. 4(a,b)). The brittle nature of these fracture surfaces is likely due to the presence of Cu–Ni and Cu–Ni–Zr rich Ti phases in the brazed joint. In contrast, ductile dimple rupture fracture is found in specimen with higher brazing temperature and longer brazing time, e.g. 990 °C for 3600 s (Fig. 4(d)). The dimple dominated fracture is usually preferred to the quasi-cleavage fracture in structural applications. It is highly recommended that Cu–Ni and Cu–Ni–Zr rich Ti phases should be minimized in the brazed joint in order to avoid brittle failure.

4. Conclusion

Infrared brazed Ti–6Al–4V and SP-700 alloys using the Ti–20Zr–20Cu–20Ni foil has been evaluated. The brazed joint consists of at least three distinctive phases, a Ti-rich phase alloyed with low Cu, Ni, Zr contents, a Cu–Ni rich Ti phase and a Cu–Ni–Zr rich Ti phase. The amount of both the Cu–Ni rich and Cu–Ni–Zr rich Ti phases is decreased with increasing the brazing temperature and/or time, and they are almost disappeared for the specimen infrared brazed at 900 °C for 3600 s. Quasi-cleavage fracture on the brazed joint is widely observed for the specimen with lower brazing temperature and time, e.g. 900 °C for 180 s and 600 s, due to the existence of Cu–Ni and Cu–Ni–Zr rich Ti phases in the brazed joint. In contrast, ductile dimple dominated fracture of the substrate is observed for the specimen with higher brazing temperature and time, e.g. 990 °C for 3600 s, and it demonstrates the highest shear strength of 483 MPa. The presence of Cu–Ni and Cu–Ni–Zr rich Ti phases are detrimental to the infrared brazed joint, and it is highly recommended that Cu–Ni and Cu–Ni–Zr rich Ti phases be avoided in order to avoid brittle failure of the joint.

References

[1] R. Roger, E.W. Collings, G. Welsch, Materials Properties Handbook: Titanium Alloys, ASM International, Materials Park, 1993.
[2] J.L. Walter, M.R. Jackson, C.T. Sims, Titanium and Its Alloys: Principles of Alloying Titanium, ASM International, Materials Park, 1988.
[3] J.R. Davis, ASM Handbook, Vol. 2: Properties and Selection: Nonferrous Alloys and Special Purpose Materials, ASM International, Materials Park, 1990.
[4] M. Schwartz, Brazing: For the Engineering Technologist, ASM International, Materials Park, 1995.
[5] D.L. Olson, T.A. Siewert, S. Liu, G.R. Edwards, ASM Handbook Volume 6: Welding, Brazing and Soldering, ASM International, Materials Park, 1990.
[6] W.R. Frick, Brazing Handbook, AWS, Miami, 1991.
[7] O. Botstein, A. Schwarzman, A. Rabinkin, Mater. Sci. Eng., A 206 (1995) 14.
[8] T. Onzawa, A. Suzumura, M.W. Ko, Weld. J. 69 (1990) 462s.
[9] S. Krishnamurthy, F.H. Froes, Int. Mater. Rev. 34 (1989) 297.
[10] D.W. Liaw, R.K. Shiue, Metall. Mater. Trans. 36A (2005) 2415.
[11] C.S. Chang, B. Jha, Weld. J. 82 (2003) 28.
[12] R.K. Shiue, S.K. Wu, C.H. Chan, Metall. Mater. Trans. 25A (2004) 3177.
[13] C.T. Chang, R.K. Shiue, C.S. Chang, Scr. Mater. 54 (2006) 853.
[14] C.T. Chang, Y.C. Du, R.K. Shiue, C.S. Chang, Mater. Sci. Eng. 420A (2006) 155.
[15] T.B. Massalski, Binary Alloy Phase Diagrams, ASM International, Materials Park, 1990.